RSC Advances

PAPER

View Article Online
View Journal | View Issue

Cite this: *RSC Adv.*, 2019, **9**, 9379

Antibody-modified reduced graphene oxide film for circulating tumor cell detection in early-stage prostate cancer patients

Binshuai Wang,† Yimeng Song,† Liyuan Ge, Shudong Zhang* and Lulin Ma*

In recent years, liquid biopsies, especially for detecting circulating tumor cells (CTCs), have received great attention for cancer diagnosis and treatment monitoring. For clinical diagnosis of prostate cancer (PCa), prostate specific antigen (PSA) has been widely used as a standard method for PCa screening. However, PSA diagnostic efficacy within early-stage PCa patients with a PSA level of 4–10 ng mL^{-1} is always controversial. Therefore, the development of new methods to assist clinical PSA diagnosis is greatly desired. Herein, we report the fabrication of antibody-modified reduced graphene oxide films, which can be used to efficiently detect CTCs in PCa patients with PSA levels of 4–10 ng mL^{-1}. The antibody-modified reduced graphene oxide (rGO) films were fabricated by spray coating reduced graphene oxide solution onto a smooth glass slide and then modifying it with anti-epithelial cell adhesion molecules (anti-EpCAMs) and anti-prostate specific membrane antigen (anti-PSMA). The rGO films exhibited an excellent ability to capture CTCs from the blood of PCa patients with PSA levels of 4–10 ng mL^{-1} and the efficiency could reach 60% (6/10). Our approach for highly efficient detection of CTCs in early-stage PCa patients may provide great potential in assisting clinical cancer diagnosis.

Received 19th October 2018
Accepted 5th March 2019

DOI: 10.1039/c8ra08682f

rsc.li/rsc-advances

1. Introduction

Prostate cancer (PCa) is one of the most common cancer types and the second leading cause of cancer-related mortality in men.[1] Serum prostate specific antigen (PSA) has been widely utilized as a screening biomarker for the diagnosis of PCa. However, its diagnostic efficacy within the PSA gray zone (PSA levels of 4–10 ng mL^{-1}) patients is still controversial which often leads to unnecessary invasive biopsies. For these patients, the positive predictive value for PCa by prostate biopsy is only 20–25%.[2] Abnormal PSA levels and negative biopsy results may cause patients psychological pressure and place clinicians in a dilemma for the disease diagnosis. Thus, there is an urgent need for the development of new methods to assist clinical PSA diagnosis for precise early stage cancer diagnosis.

Circulating tumor cells (CTCs) are regarded as a population of rare cancer cells detached from a primary tumor and/or metastatic lesions. Accumulating data suggest that CTCs can be utilized as potential non-invasive biomarkers for the diagnosis and prognosis of various types of cancer. Recent research has reported that the generation of CTCs is an important step in cancer metastasis, and CTC detection provides valuable evidence associated with disease stage and treatment monitoring.[3–5] However, CTCs are very rare in blood circulation at usually less than 10 per mL of blood. Isolating pure CTCs from billions of red blood cells and millions of white blood cells remains a challenge, seriously hindering their clinical application.[6]

In recent years, many methods have been developed for isolating CTCs relying on cellular physical properties or molecular markers. Sollier *et al.* have reported the size-selective collection of CTCs using Vortex technology.[7] Other affinity based technologies are based on the principles of CTC preferential adhesion by modifying the substrate with anti-EpCAMs. Recent advances have demonstrated that the efficient capture of CTCs can be achieved using nanostructured biointerface materials designed with a synergistic combination principle of structure match and specific molecular recognition.[8–11] Among these, Hyeun *et al.* found an effective approach (sensitivity: 73% ± 32.4 at 3–5 cells per mL of blood) to isolate and release CTCs from blood samples of pancreatic, breast and lung cancer patients, using functionalised graphene oxide nanosheets on a patterned gold surface.[12,13] On the basis of these advanced achievements, we investigate whether early stage screening of clinical PCa with PSA levels of 4–10 ng mL^{-1} can be assisted through the detection of CTCs to help us improve the diagnostic efficacy of PSA.

Here, we report the fabrication of antibody-modified reduced graphene oxide (rGO) films, which are used for the detection of circulating tumor cells in prostate cancer patients with serum PSA levels of 4–10 ng mL^{-1}. The antibody-modified rGO films were fabricated using a spray coating method and

Department of Urology, Peking University Third Hospital, Beijing 100191, China. E-mail: shootong@163.com; malulin@medmail.com.cn

† These two authors contributed equally to this work.

then surface antibody modification. We demonstrate that the rGO films exhibited an excellent ability to capture CTCs from PCa patients with PSA levels of 4–10 ng mL^{-1} with an efficiency of 60%.

2. Experimental

2.1. Fabrication of antibody-modified reduced graphene oxide films

Antibody-modified reduced graphene oxide (rGO) films were prepared by spray coating reduced graphene oxide solution onto a smooth glass slide and then, through chemical reagent activation, they were modified with anti-epithelial cell adhesion molecules (anti-EpCAMs) and anti-prostate specific membrane antigen (anti-PSMA).

In a typical fabrication, GO was dispersed in water (5 mg mL^{-1}) and was sonicated for 30 min, the pH value of which was then adjusted to ~8.5 with triethylamine. Next, an aqueous solution of 6-arm polyethylene glycol-amine (2 mg mL^{-1}) was added into the aforementioned GO solution under vigorous stirring. Subsequently, 4 mM *N*-(3-dimethylaminopropyl)-*N*-ethylcarbodiimide hydrochloride (EDC) was added to the solution, and kept stirring overnight. To prepare PEG–rGO, the above PEG–GO solution was kept at a pH value of 9–10 with triethylamine. Then, a freshly prepared sodium borohydride solution (10 mg mL^{-1}) was added to the above solution under vigorous stirring. The reaction mixture was kept stirring at 80 °C for 2 h. During the reduction, the dispersion turned black, accompanied by outgassing. The final mixture was treated with an ultrasonic probe at 200 W for 1 h, followed by sonication for 2 h. The mixture was filtrated and centrifuged repeatedly, resulting in a PEG–rGO solution with a pH ≈ 7. This isolated PEG–rGO composite was then filtrated and dried to yield a powder (83%). The films were prepared by spray coating onto the surface of a smooth glass slide (1 × 2 cm). Smooth glass slides (flat films) were used as negative controls.

In a typical functionalization, pyrene carboxylic acid (PCA) (3 mg mL^{-1} in methanol) was immobilized onto PEG–rGO film for 24 h and then dried with nitrogen gas. 3 mL of streptavidin was conjugated onto the PCA–PEG–rGO film *via* an immobilization procedure over 1 h assisted by 3 mL of a solution of *N*-hydroxysulfosuccinimide (sulfo-NHS) and *N*-(3-dimethylaminopropyl)-*N*-ethylcarbodiimide hydrochloride (EDC) for 1.5 h. 25 μL of biotinylated anti-EpCAM and anti-PSMA (pre-warmed at 37 °C) was immobilized onto the SA–PEG–rGO film which was incubated at 37 °C for 30 min. The flat glass films also underwent the same steps mentioned above.[14]

2.2. Cell culture and capture

Human PCa cell lines PC3 and 22Rv1, a Daudi Burkitt cell line and a Jurkat T lymphocyte cell line were purchased from the China Center for Type Culture Collection (Shanghai, China). Cells were maintained in RPMI1640 medium (22Rv1, Daudi and Jurkat) and F-12K medium (PC3) supplemented with 10% fetal bovine serum and 1% penicillin/streptomycin solution at 37 °C in a 5% CO_2 incubator. The cells were harvested for experiments at 80–90% confluence. Anti-EpCAM and anti-PSMA modified rGO films and flat films were placed into four-well cell culture plates (Lab-Tek II, Chamber Slide, USA). The cell suspensions (1 mL of 50, 100, 200 and 500 cells per mL) were carefully added into each well and incubated in incubators (37 °C, 5% CO_2) for 30 min. The device for counting cells was homemade with a stretched glass capillary connected to a blood collection tube and injector. Afterwards, the films were taken out of the cell suspensions and rinsed carefully three times with PBS. After the cells were fixed using paraformaldehyde solution, penetrated using Triton-X100, and dyed using DAPI solution (2 mg mL^{-1} in water), the captured cells were counted using fluorescence microscopy (Nikon, Ti-E, Tokyo, Japan). The experiments were repeated three times.

2.3. Patient selection and blood capture procedure

All experiments were performed in accordance with the guidelines "Ethics of Biomedical Research with Human Involved (National Health Commission of P. R. China)". The experiments were approved by the ethics committee of Peking University Third Hospital. Informed consent was obtained from human participants in this study. 4 metastatic castration-resistant prostate cancer (mCRPC) patients and 10 prostate cancer patients with PSA levels of 4–10 ng mL^{-1} were enrolled in this study. 4 mL of fresh blood was taken once the pathological results were confirmed to be prostate cancer for CTC detection. Samples of blood (4 mL) were drawn into ethylenediaminetetraacetic acid (EDTA) tubes and stored for a maximum of 4 h at 4 °C before processing. Anti-EpCAM and anti-PSMA-modified rGO films were placed into culture plates. 4 mL of fresh blood was divided equally into four samples. The capture steps were the same as those mentioned above. Cells captured on the substrate were identified using a typical three-color immunostaining method. After fixation, permeabilization and blocking, the cells were stained with a mixed PE-labeled anti-CK and an FITC-labeled anti-CD45 solution at 4 °C overnight in the dark, washed with PBS three times (5 min each) and incubated with DAPI for 5 min. After three washes, the samples were taken for fluorescence imaging (Fig. 1).

2.4. Environmental scanning electron microscopy (ESEM) imaging

We used PC3, 22Rv1 and the mCRPC patients' blood samples for detecting the interaction between the cancer cells and the rGO film interface. In addition, we also used the PC3 cell line for evaluating the interaction and efficiency differences between the rGO films and the flat films. The cell captured films were washed 3 times with PBS and fixed in 2.5% glutaraldehyde solution overnight. Dehydration with ethanol of different concentrations (30%, 50%, 60%, 90%, 95% and 100%) was then performed. The substrates were treated with 50% ethanol and 100% hexamethyldisilazane for 10 min, in sequence. After gold sputtering, the films were observed under an environmental scanning electron microscope (Hitachi, Japan).

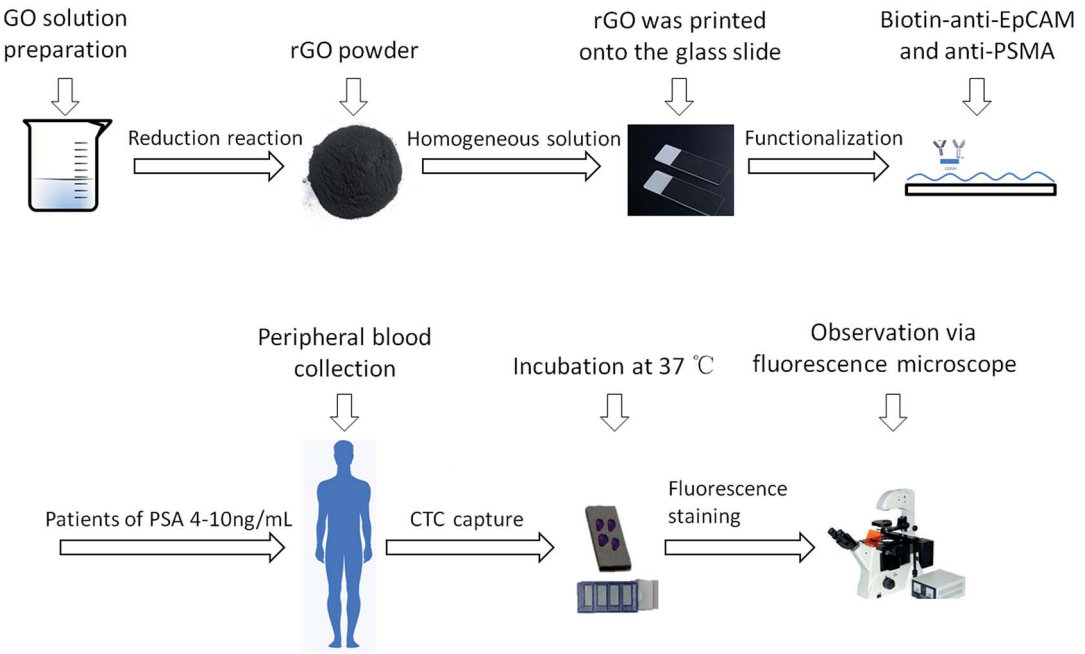

Fig. 1 Flow chart of rGO film fabrication and blood CTC detection. GO was reduced to rGO and rGO was printed onto glass slides as rGO film. The rGO films were functionalized using anti-EpCAM and anti-PSMA and were used for CTC detection in patients with PSA levels of 4–10 ng mL^{-1}.

3. Results and discussion

3.1. rGO film features and cell capture

Nowadays, many cell–material interactions are mediated by bioactive interfaces based on chemical or physical aspects of cell behavior. These interactions include cell adhesion, geometry-controlled cell fate and topography-guided stem cell differentiation.[15–17] Nonetheless, the functions performed by these artificial biointerfaces are far simpler than those in the natural cell microenvironment which include the use of surface topography and chemistry, matrix stiffness, mechanical stress, and other parameters. These problems present a major challenge for designing biointerfaces that can incorporate several biophysical cell properties to achieve cell-specific recognition and avoid non-specific adhesion.

The first step in this study was the fabrication of rGO films. The rGO films were prepared *via* a two-step process involving a reduction reaction and printing process. The negative charge and super hydrophilicity of reduced graphene oxide renders the surface inert to nonspecific cell adhesion. The rough texture of rGO film might enhance the topographic interactions between CTCs and biointerfaces. Moreover, the low stiffness of the rGO films might contribute to improving the efficiency of CTC capture.

A representative image of a prepared sample is shown in Fig. 2B. The rGO films exhibited a petal-like wrinkled architecture compared to the flat films (Fig. 2A). A more detailed image is shown in Fig. 2C and D. The petal-like wrinkled architecture improves the interfacial interactions with cells and provides sites for cell filopodia binding. Films with rougher surfaces exhibited greater cell spreading and filopodia that were more elongated (Fig. 2F–H). The cancer cells exhibited extremely long protrusions along the wrinkles which indicated that the cancer cells are more likely to grasp a rough surface than smoother substrates (Fig. 2E) due to the synergy of the topographic interactions included in the nanostructure-induced matching effect and the antibody-induced binding effect.

3.2. The CTC capture efficiency of the rGO films

CTCs are present in the bloodstream at very low concentrations. Various methods have been generated for CTC isolation including the Cell Search® platform and several nanomaterial-based biointerfaces which have lower accuracy and sensitivity.[18] In the present study, we have developed a new optimized rGO film by mimicking topographic features to realize highly efficient detection of CTCs. Several other studies have showed that prostate specific membrane antigen (PSMA) is overexpressed in prostate cancer and represents an excellent cell surface protein for targeted therapy. In the current study, the rGO films modified with anti-EpCAM and an anti-PSMA antibody were expected to improve the efficiency of CTC capture.

To test the capture efficiency of the rGO films, we spiked different types of serial number in 1640 medium as a model system to verify the capture efficiency between the antibody-modified rGO films and the flat films. As shown in Fig. 3A, PC3 cells were captured with an efficiency of 81.2 ± 4.8% by the rGO film, whereas the capture efficiency of the flat film was only 15.7 ± 2.3%. The capture efficiencies of molecular marker positive cell lines (PC3 and 22Rv1) were 84.1 ± 2.1% and 79.4 ± 3.5% which were higher than those of the negative control cell

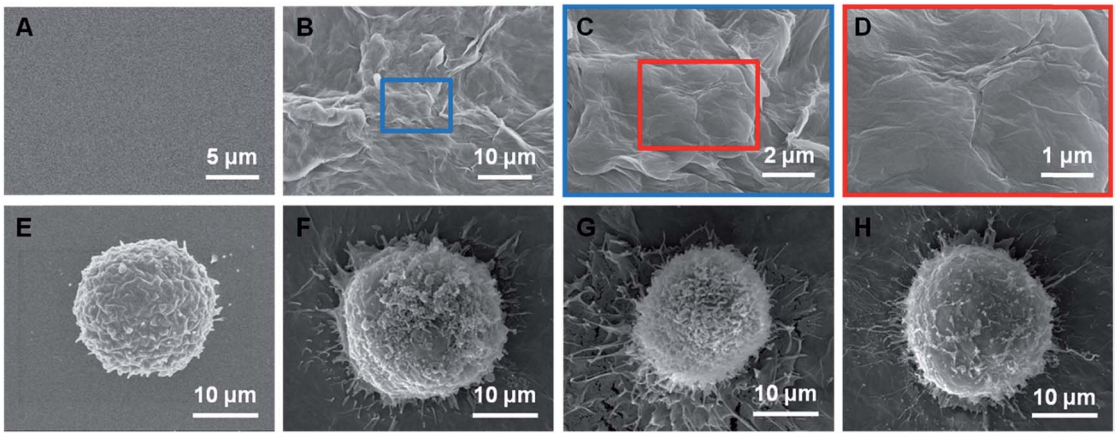

Fig. 2 (A and E) ESEM images of the flat films with surfaces which do not have a microstructure and the PC3 cell, which displayed a spherical shape and does not have enough filopodia. (B–D) ESEM images of the rGO film surface which clearly show the existence of a petal-like wrinkled architecture. (F–H) The attachment relationship between a 22Rv1 cell, a PC3 cell and an mCRPC cell and the functional surface with the cell shape changed and the appearance of filopodia.

lines (Daudi and Jurkat) of 15.1 ± 2.3% and 16.1 ± 2.1% (Fig. 3B). We also demonstrated that the rGO films showed steady and reliable collection of PC3 cells with a linear relationship ($R^2 = 0.9995$) (Fig. 3C).

3.3. Patient characteristics and CTC detection

PSA screening is the main method for the diagnosis of PCa, but has a low specificity for early-stage PCa. As a result, prostate biopsies remain the gold standard test for definitive PCa

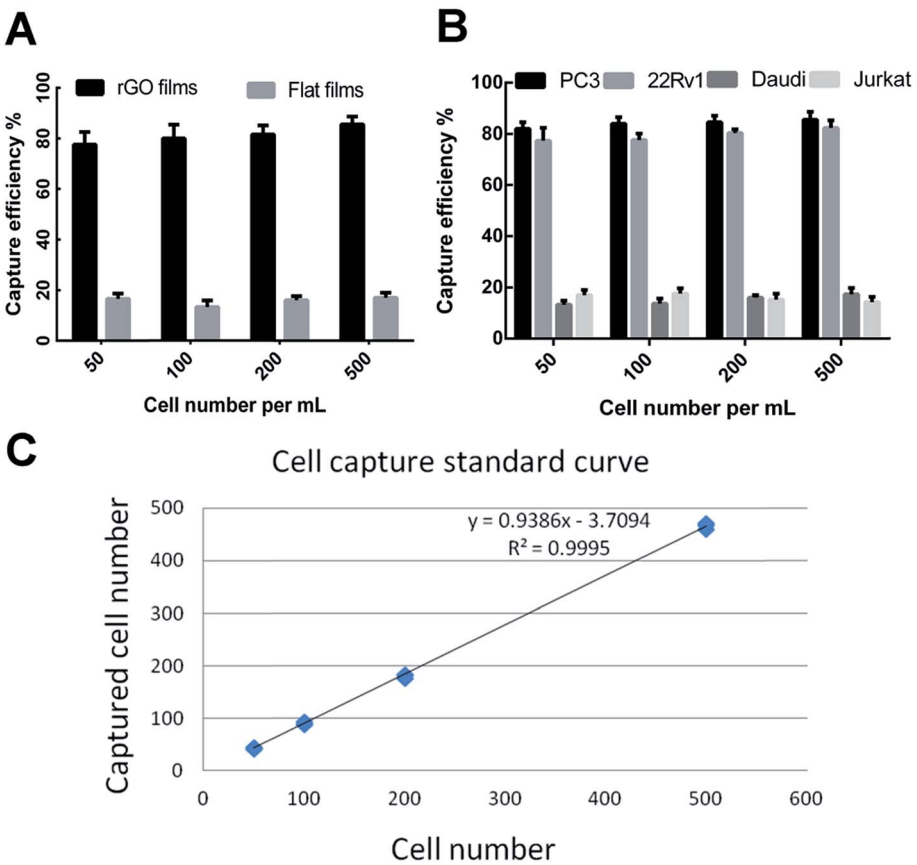

Fig. 3 (A) The capture efficiency for the PC3 cell line on rGO films and flat films. (B) The capture efficiency of PC3, 22Rv1, Daudi and Jurkat on anti-EpCAM- and anti-PSMA-modified films. (C) The capture efficiency of PC3 had a cell number-dependent linear relationship with $R^2 = 0.9995$.

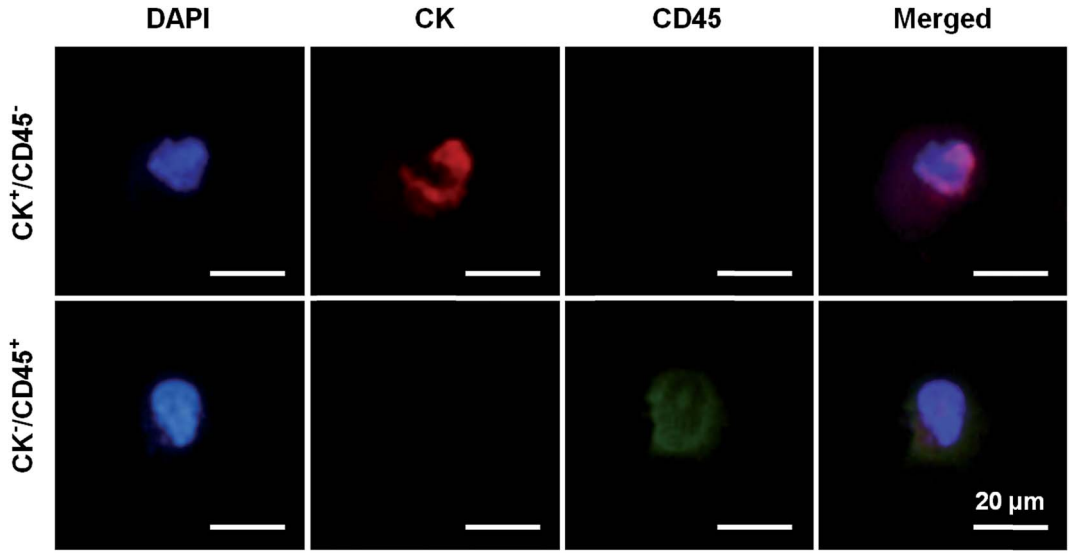

Fig. 4 Immunofluorescence staining images, where $CK^+/CD45^-$ represents the CTC of a PCa patient and $CK^-/CD45^+$ represents the white blood cell of a PCa patient.

diagnosis. However, previous studies have reported that the rate of PCa detection after biopsies in men with PSA levels of 4.0–10.0 ng mL^{-1} was only 20–25%.[2] Subsequently, many auxiliary detection methods have been developed to improve the accuracy of diagnosis including total PSA, free/total PSA, PSA velocity (PSAV) and PSA density (PSAD).[19–21] Meanwhile, although CTCs have been recently accepted as prognostic markers in metastatic PCa, very few studies have analyzed their role in early-stage PCa. CTCs provide the ability to take a "liquid biopsy" and represent a noninvasive tool for obtaining tumor samples at different time points, thereby allowing physicians to validate therapeutic decisions and obtain actual information about the cancer phenotype.[22,23] In addition, the application of CTC counts in the diagnosis of early prostate cancer is not ideal. Davis *et al.* found that CTCs can be detected in only 5% of patients with localized prostate cancer, and CTC counts are not associated with tumor volume, pathological stage, or Gleason score.[24] CTCs were detected in 20 patients with high-risk localized prostate cancer using the CellSearch system and the results showed that only one CTC-positive patient was detected.[25] Summary studies have found that the positive rate of CTC detection in patients with early-stage prostate cancer is 5–52%.[26–29] Herein, the present study was initiated due to the lack of data on the presence of CTCs in the diagnosis of prostate cancer. We aimed to evaluate the efficacy of the antibody-modified reduced graphene oxide film technique for detecting CTCs in early-stage prostate cancer patients.

Prostate biopsy results and clinical characteristics were available for 4 mCRPC patients and 10 patients with PSA levels of 4–10 ng mL^{-1}. The pathology results reported that all the

Table 1 Clinical features and CTC detection results of all the prostate cancer patients

Patients	Serum PSA degree (ng mL^{-1})	TNM stage[a]	Metastasis site[b]	CTC positive
mCRPC 1	44.32	T3N1M1	Bone	+
mCRPC 2	36.24	T3N0M1	Bone	+
mCRPC 3	23.58	T3N0M1	Bone	+
mCRPC 4	22.67	T2N0M1	Bone	+
PSA gray zone 1	9.42	T1N0M0	Not detected	+
PSA gray zone 2	8.84	T2N0M0	Not detected	+
PSA gray zone 3	8.72	T2N0M0	Not detected	+
PSA gray zone 4	7.57	T1N0M0	Not detected	+
PSA gray zone 5	7.46	T1N0M0	Not detected	−
PSA gray zone 6	7.43	T1N0M0	Not detected	+
PSA gray zone 7	7.38	T1N0M0	Not detected	+
PSA gray zone 8	7.34	T1N0M0	Not detected	−
PSA gray zone 9	6.99	T1N0M0	Not detected	−
PSA gray zone 10	6.69	T1N0M0	Not detected	−

[a] The TNM stage was determined using International Union Against Cancer, 8th edition. [b] The metastasis site was determined through medical imaging examination.

patients had prostate adenocarcinoma. The patients' blood samples were processed on the anti-EpCAM and anti-PSMA rGO films for CTC capture. We defined that if the cell had positive CK and DAPI staining but negative CD45 staining it was a CTC cell and that the cell nuclear-cytoplasmic ratio also should be over 50%. In contrast, white blood cells would have negative CK and positive CD45 staining (Fig. 4). 2 or more CTCs/4 mL of blood was used as the cut-off value to determine CTC positivity in samples. All of the 4 mCRPC patients were CTC positive which indicated that the rGO film had the ability to capture CTCs from advanced-stage prostate cancer patients. Afterwards, the rGO film was used for CTC detection from patients with PSA levels of 4–10 ng mL^{-1} and 6 out of 10 (60%) patients were CTC positive which indicated that the rGO film also had the ability to capture CTCs from early-stage patients and this was significantly higher than in existing research. All this information is summarized in Table 1.

4. Conclusion

In conclusion, we demonstrated the fabrication of an antibody-modified rGO film and realized highly efficient capture of CTCs from PCa patients with PSA levels of 4–10 ng mL^{-1}. The antibody-modified rGO film was fabricated using a spray coating method and surface antibody modification. The obtained antibody-modified rGO film exhibited significant capacity for capturing PC3 and 22Rv1 cells with the very high efficiencies of 84.1 $\pm$ 2.1% and 79.4 $\pm$ 3.5%. On the basis of these results, we further demonstrated that for early-stage PCa, the sensitive isolation of CTCs using an antibody-modified reduced graphene oxide film is feasible with a capture efficiency of 60%. This ability to detect CTCs in prostate cancer patients with PSA levels of 4–10 ng mL^{-1} reveals the potential for this to be used as a novel screening method for the diagnosis of prostate cancer.

Conflicts of interest

There are no conflicts to declare.

Acknowledgements

The research is supported by the Beijing Municipal Science and Technology Commission (Z161100000116037).

References

1 R. L. Siegel, K. D. Miller and A. Jemal, *Ca-Cancer J. Clin.*, 2018, **68**, 7–30.
2 Y. Zhou, Y. Li, X. Li and M. Jiang, *BioMed Res. Int.*, 2017, **2017**, 2512536.
3 G. T. Budd, M. Cristofanilli, M. J. Ellis, A. Stopeck, E. Borden, M. C. Miller, J. Matera, M. Repollet, G. V. Doyle, L. W. Terstappen and D. F. Hayes, *Clin. Cancer Res.*, 2006, **12**, 6403–6409.
4 M. Cristofanilli, G. T. Budd, M. J. Ellis, A. Stopeck, J. Matera, M. C. Miller, J. M. Reuben, G. V. Doyle, W. J. Allard, L. W. Terstappen and D. F. Hayes, *N. Engl. J. Med.*, 2004, **351**, 781–791.
5 D. F. Hayes, M. Cristofanilli, G. T. Budd, M. J. Ellis, A. Stopeck, M. C. Miller, J. Matera, W. J. Allard, G. V. Doyle and L. W. Terstappen, *Clin. Cancer Res.*, 2006, **12**, 4218–4224.
6 H. W. Hou, M. E. Warkiani, B. L. Khoo, Z. R. Li, R. A. Soo, D. S. Tan, W. T. Lim, J. Han, A. A. Bhagat and C. T. Lim, *Sci. Rep.*, 2013, **3**, 1259.
7 E. Sollier, D. E. Go, J. Che, D. R. Gossett, S. O'Byrne, W. M. Weaver, N. Kummer, M. Rettig, J. Goldman, N. Nickols, S. McCloskey, R. P. Kulkarni and D. Di Carlo, *Lab Chip*, 2014, **14**, 63–77.
8 S. Wang, H. Wang, J. Jiao, K. J. Chen, G. E. Owens, K. Kamei, J. Sun, D. J. Sherman, C. P. Behrenbruch, H. Wu and H. R. Tseng, *Angew. Chem., Int. Ed. Engl.*, 2009, **48**, 8970–8973.
9 H. Cui, B. Wang, W. Wang, Y. Hao, C. Liu, K. Song, S. Zhang and S. Wang, *ACS Appl. Mater. Interfaces*, 2018, **10**, 19545–19553.
10 Y. Li, Q. Lu, H. Liu, J. Wang, P. Zhang, H. Liang, L. Jiang and S. Wang, *Adv. Mater.*, 2015, **27**, 6848–6854.
11 S. Wang, K. Liu, J. Liu, Z. T. Yu, X. Xu, L. Zhao, T. Lee, E. K. Lee, J. Reiss, Y. K. Lee, L. W. Chung, J. Huang, M. Rettig, D. Seligson, K. N. Duraiswamy, C. K. Shen and H. R. Tseng, *Angew. Chem., Int. Ed. Engl.*, 2011, **50**, 3084–3088.
12 H. J. Yoon, T. H. Kim, Z. Zhang, E. Azizi, T. M. Pham, C. Paoletti, J. Lin, N. Ramnath, M. S. Wicha, D. F. Hayes, D. M. Simeone and S. Nagrath, *Nat. Nanotechnol.*, 2013, **8**, 735–741.
13 H. J. Yoon, A. Shanker, Y. Wang, M. Kozminsky, Q. Jin, N. Palanisamy, M. L. Burness, E. Azizi, D. M. Simeone, M. S. Wicha, J. Kim and S. Nagrath, *Adv. Mater.*, 2016, **28**, 4891–4897.
14 W. Wang, G. Yang, H. Cui, J. Meng, S. Wang and L. Jiang, *Adv. Healthcare Mater.*, 2017, **6**(15), 1700003.
15 S. Petersen, J. M. Alonso, A. Specht, P. Duodu, M. Goeldner and A. del Campo, *Angew. Chem., Int. Ed. Engl.*, 2008, **47**, 3192–3195.
16 C. S. Chen, M. Mrksich, S. Huang, G. M. Whitesides and D. E. Ingber, *Science*, 1997, **276**, 1425–1428.
17 C. J. Bettinger, R. Langer and J. T. Borenstein, *Angew. Chem., Int. Ed. Engl.*, 2009, **48**, 5406–5415.
18 K. Pantel, E. Deneve, D. Nocca, A. Coffy, J. P. Vendrell, T. Maudelonde, S. Riethdorf and C. Alix-Panabieres, *Clin. Chem.*, 2012, **58**, 936–940.
19 A. W. Roddam, M. J. Duffy, F. C. Hamdy, A. M. Ward, J. Patnick, C. P. Price, J. Rimmer, C. Sturgeon, P. White, N. E. Allen and N. H. S. P. C. R. M. Programme, *Eur. Urol.*, 2005, **48**, 386–399; discussion 398–389.
20 A. E. Pelzer, H. Volgger, J. Bektic, A. P. Berger, P. Rehder, G. Bartsch and W. Horninger, *BJU Int.*, 2005, **96**, 995–998.
21 Y. Kobori, Y. Kitagawa, A. Mizokami, K. Komatsu and M. Namiki, *Int. J. Clin. Oncol.*, 2008, **13**, 229–232.
22 P. Paterlini-Brechot and N. L. Benali, *Cancer Lett.*, 2007, **253**, 180–204.

23 B. Hu, H. Rochefort and A. Goldkorn, *Cancers*, 2013, **5**, 1676–1690.
24 J. W. Davis, H. Nakanishi, V. S. Kumar, V. A. Bhadkamkar, R. McCormack, H. A. Fritsche, B. Handy, T. Gornet and R. J. Babaian, *J. Urol.*, 2008, **179**, 2187–2191; discussion 2191.
25 M. Thalgott, B. Rack, T. Maurer, M. Souvatzoglou, M. Eiber, V. Kress, M. M. Heck, U. Andergassen, R. Nawroth, J. E. Gschwend and M. Retz, *J. Cancer Res. Clin. Oncol.*, 2013, **139**, 755–763.
26 S. L. Stott, R. J. Lee, S. Nagrath, M. Yu, D. T. Miyamoto, L. Ulkus, E. J. Inserra, M. Ulman, S. Springer, Z. Nakamura, A. L. Moore, D. I. Tsukrov, M. E. Kempner, D. M. Dahl, C. L. Wu, A. J. Iafrate, M. R. Smith, R. G. Tompkins, L. V. Sequist, M. Toner, D. A. Haber and S. Maheswaran, *Sci. Transl. Med.*, 2010, **2**, 25ra23.
27 K. Kolostova, M. Broul, J. Schraml, M. Cegan, R. Matkowski, M. Fiutowski and V. Bobek, *Anticancer Res.*, 2014, **34**, 3641–3646.
28 S. K. Pal, M. He, T. Wilson, X. Liu, K. Zhang, C. Carmichael, A. Torres, S. Hernandez, C. Lau, N. Agarwal, M. Kawachi, Y. Yen and J. O. Jones, *Clin. Genitourin. Cancer*, 2015, **13**, 130–136.
29 C. P. Meyer, K. Pantel, P. Tennstedt, P. Stroelin, T. Schlomm, H. Heinzer, S. Riethdorf and T. Steuber, *Urol. Oncol.*, 2016, **34**, 235–236.